

On the Repeatability of EEG Features in a Biometric Recognition Framework using a Resting State Protocol

Daria La Rocca¹, Patrizio Campisi¹ and Gaetano Scarano²

¹Department of Applied Electronics, Università degli Studi "Roma Tre", via Della Vasca Navale 84, I-00146 Roma, Italy

²DIET, Sapienza Università di Roma, via Eudossiana 18, I-00184 Roma, Italy

Keywords: EEG, Biometrics, Repeatability, Resting.

Abstract: In this paper the feasibility of the electroencephalogram (EEG) as biometric identifier is investigated with focus on the repeatability of the EEG features employed in the proposed framework. The use of EEG within the biometric framework has already been introduced in the recent past although it has not been extensively analyzed. In this contribution we infer about the invariance over time of the employed EEG features, which is one of the most relevant properties a biometric identifier should possess in order to be employed in real life applications. For the purpose of this study we rely on the "resting state" protocol. The employed database is composed by healthy subjects whose EEG signals have been acquired in two different sessions. Different electrodes configurations pertinent to the employed protocol have been considered. Autoregressive statistical modeling using reflection coefficients has been adopted and a linear classifier has been tested. The obtained results show that a high degree of repeatability has been achieved over the considered interval.

1 EEG AS BIOMETRICS

From the beginning of the 20th century, EEG analysis has been mainly used in medicine to study brain diseases like Alzheimer, epilepsy, Parkinson and many others. Specifically, EEG signals, acquired by means of scalp electrodes, sense the electrical activity related to the firing of specific collections of neurons responding to a variety of cognitive tasks such as audio or visual stimuli, real or imagined body movements, imagined speech, etc. The most relevant cerebral activities falls in the range of [0.5, 40] Hz. In details five wave categories have been identified, each associated to a specific bandwidth and to specific cognitive tasks: *delta waves* (δ) [0.5, 4]Hz which are primarily associated with deep sleep, loss of body awareness, and may be present in the waking state; *theta waves* (θ) [4, 8]Hz which are associated with deep meditation and creative inspiration; *alpha waves* (α) [8, 13]Hz which indicate either a relaxed awareness without any attention or concentration; *beta waves* (β) [13, 30]Hz usually associated to active thinking; *gamma waves* (γ) [30, 40]Hz usually used to locate right and left movements.

In the last decades, the brain activity, registered by means of EEG, has been heavily employed in brain computer interfaces (BCI) (Dornhege et al., 2007)

and more recently in brain machine interface (BMI) (Carmena, 2012) for prosthetic devices. In the last few years EEG signals have also been proposed to be used in biometric based recognition systems (Campisi et al., 2012).

EEG signals present some peculiarities, which are not shared by the most commonly used biometrics, like face, iris, and fingerprints. Specifically, brain signals generated on the cortex are not exposed like face, iris, and fingerprints, therefore they are more privacy compliant than other biometrics since they are "secret" by their nature, being impossible to capture them at a distance. This property makes EEG biometrics also robust against the spoofing attack at the sensor since an attacker would not be able to collect and feed the EEG signals. Moreover, being brain signals the result of cognitive processes, they cannot be synthetically generated and fed to a sensor, which also addresses the problem of liveness detection. Also, the level of universality of brain signals is very high. In fact people with some physical disabilities, preventing the use of biometrics like fingerprint or iris, would be able to get access to the required service using EEG biometrics. However, the level of understanding of the physiological mechanisms behind the generation of electric currents in the brain, not yet fully got, makes EEG a biometrics at its embryonic stage. Nev-

Table 1: State of the art on EEG biometrics using a resting state protocol.

Paper	Protocol	# Subj	# Ch.	Features
(Poulos et al., 1999)	CE	4	1	AR (6th)
(Campisi et al., 2011)	CE	48	3	AR (6th)
(Paranjape et al., 2001)	CE, OE	40	1	AR (21th)
(Palaniappan and Patnaik, 2007)	CE	5	6	AR (6th)
(Zhao et al., 2010)	CE	10	1	AR (6th) + PSD
(Abdullah et al., 2010)	CE, OE	10	4	AR (21th)
(Mohammadi et al., 2006)	OE	10	2-3	AR (11th)
(Nakanishi et al., 2009)	CE	23	1	FFT

ertheless, some preliminary, but promising, results have already been obtained in the recent literature, see for example (Poulos et al., 1999), (Brigham and Kumar, 2010), (Riera et al.,), (Marcel and del R. Millan, 2007), (Campisi et al., 2011) where a review on the state of the art of EEG biometrics is also given, and (La Rocca et al., 2012). Due to the early stage of research dealing with EEG as biometrics, currently, the deployment of convenient and accurate EEG based applications in real world are limited with respect to well established biometrics like fingerprints, iris, and face. However the brain electrical activity has already shown some potentials to allow automatic user recognition. Answers to practical and theoretical questions addressed for the development of a usable system can be found in (Su et al., 2010) where promising results are obtained from the implementation of a portable EEG biometric framework for applications in real world scenarios. Improvements in EEG signal acquisition and technological advances in the use of wireless and dry sensors, easy to wear and robust with respect to noise (Debener et al., 2012) could represent the cue for outlining guidelines for practical systems implementation.

In Table 1, an extensive although not exhaustive list of research studies which have already been published using a resting state acquisition protocol, either closed eyes (CE) or open eyes (OE), is provided. It is evident that the database dimension is quite limited in almost all of these contributions. This is also due to the lack of a public EEG database suitably collected for the biometric recognition purpose, where acquisitions and protocols would be designed according to the specific requirements. In fact most of the works in this field test the implemented techniques on datasets recorded in BCI contexts. Moreover the issue of the repeatability of EEG biometrics in different acquisition sessions has never been systematically addressed in any of the aforementioned contributions and it has never received the required attention from the scientific community. Nevertheless, its understanding is

propaedeutic towards the deployment of EEG biometrics in real life. Although in some referred works different acquisition sessions have been provided, they were considered to assort a single dataset where randomly selected EEG segments were used for training or testing a classification algorithm for the recognition purpose. On the other hand, in (Brigham and Kumar, 2010) the session-to-session variability was tested on a dataset of 6 subjects performing imagined speech. The entire set of 128 channels was used to extract features, and results show a decreasing performance when considering sessions temporally apart, which led to assess that the imagined speech EEG does not show to have a reliable degree of repeatability. Therefore, in this paper we further speculate on the use of EEG as a biometric characteristic by focusing on the analysis of repeatability of its features, thus starting filling a gap in the existing literature. More in details, we rely on two simple acquisition protocols, namely “resting states with eyes open” and “resting states with eyes closed” to acquire data from nine healthy subjects in two acquisition sessions separated in time. Different configurations for the number of electrodes employed and for their spatial placement have been taken into account. Specifically, sets of three and five electrodes have been considered to acquire the signals, and several frequency bands have been analyzed. The so acquired signals, after proper preprocessing, are then modeled using autoregressive stochastic modeling in the feature extraction stage. Linear classification is then performed. The paper is organized as follows. The acquisition protocol is detailed in Section 2, and in Section 3 the template extraction procedure is described. In Section 4 classification is performed, while experimental results are given in Section 5. Finally conclusions are drawn in Section 6.

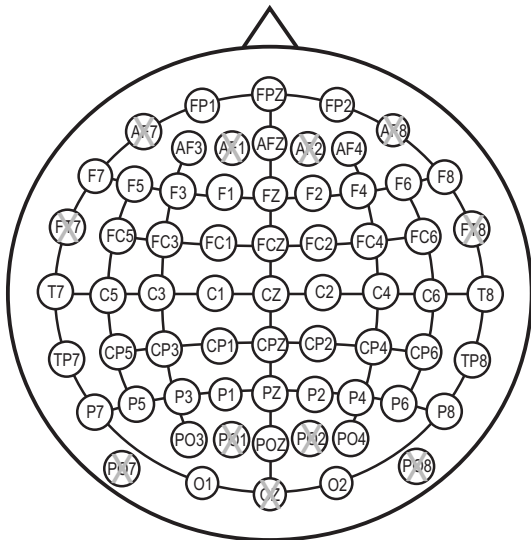


Figure 1: Scalp electrodes positioning in the employed protocol according to an extension of the standard 10-20 montage.

2 EMPLOYED ACQUISITION PROTOCOL

Nine healthy volunteers have been recruited for this experiment. Informed consent was obtained from each subject after the explanation of the study, which was approved by the local institutional ethical committee. During the experiment, the participants were comfortably seated in a reclining chair with both arms resting on a pillow in a dimly lit room properly designed minimizing external sounds and noise in order not to interfere with the attention and the relaxed state of subjects. The subjects were asked to perform one minute of “resting state with eyes open” and one minute of “resting state with eyes closed” (Barry et al., 2007) in two temporally separated sessions, from 1 to 3 weeks distant from each other, depending on the subject. Brain activity has been recorded using a BrainAmp EEG recording system operating at a sampling rate of 200 Hz. The EEG was continuously recorded from 54 sites positioned according to the International 10-20 system as shown in Figure 1. Such configuration is not meant to be a user convenient solution, but allows to investigate about a proper electrode placement, able to catch distinctive features according to the employed protocol. Before starting the recording session, the electrical impedance of each electrode was kept lower than 10 kOhm through a dedicated gel maximizing the skin contact and allowing for a low-resistance recording through the skin. After the EEG recording sessions, the EEG signals

have been band pass filtered in the band $[0.5, 30]$ Hz. In addition, a preprocessing has been applied to improve the signal-to-noise ratio (SNR), as described in Section 3.1.

3 TEMPLATE EXTRACTION

The template is generated by considering the signals acquired by a properly chosen set of electrodes. We have tested different acquisition configurations. Specifically, sets of three and five electrodes have been employed in our tests to understand, at a first stage, the proper number of electrodes to employ, limiting it, and at a later stage, the proper electrodes positioning to use in order to capture repeatable and stable features, if present. The signals so acquired are preprocessed as described in Section 3.1 in order to perform denoising and to select the proper subbands. Then, the EEG signals in the selected subbands are AR modeled as described in Section 3.2. The template is obtained by concatenating the reflection coefficients vectors related to the different channels in the sets under analysis. Specific brain rhythms are mainly predominant in certain scalp regions during different mental states. Therefore, we expected a certain variability of recognition performance spanning the entire scalp through specific configurations of electrodes, and considering the closed or open eyes condition, being different the capability to catch distinctive features.

3.1 Preprocessing

Before performing feature extraction, each acquired raw EEG signal has been processed as described in the following. Neural activity reflected in resting state EEG signals shows to contain frequency elements mainly below 30Hz. Hence, a decimation factor has been applied to the collected raw signals, after filtering them through an anti-aliasing FIR filter. A sampling rate of $S_r = 60\text{Hz}$ was selected to retain spectral information present in the four major EEG subbands referring to the resting state (δ $[0.5, 4]\text{Hz}$, θ $[4, 8]\text{Hz}$, α $[8, 13]\text{Hz}$ and β $[13, 30]\text{Hz}$). The γ subband $[30, 40]\text{Hz}$ is not considered, given that it is known not to be relevant in a resting condition. A further stage of zero-phase frequency filtering was applied to discriminate the different EEG rhythms. The single δ , θ , α and β subbands and their combinations (frequency components from 0.5Hz up to 30Hz, and from 0.5Hz up to 14Hz) have been considered in our experiments.

A spatial filter has been then applied to the acquired signals. When sufficiently large numbers of

electrodes are employed, potential at each location may be measured with respect to the average of all potentials, approximating an inactive reference. Specifically, a common average referencing (CAR) filter has been employed in the herein proposed analysis by subtracting the mean of the entire $C_T = 54$ electrodes montage (*i.e.* the common average) from the channel c of interest, with $c = 1, 2, \dots, C_T$, at any one instant, according to the formula:

$${}^{CAR}V_u^c[n] = V_u^c[n] - \frac{1}{C_T} \sum_{j=1}^{C_T} V_u^j[n], \quad (1)$$

where $V_u^j[n]$ is the potential between the j -th electrode and the reference electrode, for the user u , with $u = 1, 2, \dots, U$. CAR filtering has been employed to reduce artifacts related to inappropriate reference choices in monopolar recordings (Schwartz and Andrasik, 2003) or not expected reference variations, as well as to provide measures as independent as possible from the recording session. This results in an increased signal-to-noise ratio, since artifacts related to a single reference electrode are better controlled, as showed in (McFarland et al., 1997), where authors compared spatial filter methods with a conventional ear reference in an EEG-based system.

A set of instances to be used for the training and the testing stages has been obtained from the signal segmentation. A range from 1 up to 3 seconds of EEG frame length has been spanned stepwise, in order to best characterize each user brain signal for the identification purpose. The one second frame length has been experimentally selected as it has shown to best catch distinctive features of users' EEG segments for the recognition purpose. This can be observed in Figure 2, where best performance is achieved both for sets of three and five electrodes, considering one second EEG segments, in the band $\delta \cup \theta \cup \alpha \cup \beta = [0.5, 30]$ Hz shown to be the best performing. These results refer to 10 order AR modeling and best sets of three and five channels, and show averaged performance obtained training the classifier on each acquisition session and testing it on the other one. Such framework has been employed to increase the number of trials used to study the repeatability of EEG biometrics in terms of recognition performance over the investigated period.

In this stage an overlap interval between adjacent frames was set to increase the sample size. Overlapping percentages of 25%, 50% and 75% have been tested. Subsequently the DC component jointly to the linear trend has been removed from each EEG segment. The so obtained data-set have been further processed to extract the distinctive features from each user brain signal, as described below.

3.2 Modeling and Feature Vector

After the preprocessing stage, detailed in Section 3.1, each acquired signal is modeled as a realization of an AR stochastic process. A realization $x[n]$ of an AR process, of order Q , can be expressed as:

$$x[n] = - \sum_{q=1}^Q a_{Q,q} \cdot x[n-q] + w[n] \quad (2)$$

where $w[n]$ is a realization of a white noise process of variance σ_Q^2 , and $a_{Q,q}$ are the autoregressive coefficients. The well known Yule-Walker equations (Kay, 1988), which allow calculating the Q coefficients, can be solved recursively, employing the Levinson algorithm and introducing the concept of reflection coefficients. Specifically:

$$\begin{cases} a_{Q,q} = a_{Q-1,q} + K_Q \cdot a_{Q-1,Q-q}, & q = 1, \dots, Q-1 \\ \sigma_Q^2 = \sigma_{Q-1}^2 (1 - K_Q^2), \end{cases} \quad (3)$$

where the factor K_Q is the so-called *reflection coefficient* of order Q which is calculated as follows (Kay, 1988):

$$K_Q = - \left(R_x[Q] + \sum_{q=1}^{Q-1} R_x[q] \cdot a_{Q-1,Q-q} \right) / \sigma_{Q-1}^2 \quad (4)$$

where the generic $R_x[m]$ is the signal autocorrelation function, defined as $R_x[m] = E \{x[n]x[n-m]\}$, for all $m \geq 0$.

Among the possible estimation approaches, the Burg method (Kay, 1988) estimates the reflection coefficients K_q , for $q = 1, \dots, Q$, operating directly on the observed data $x[n]$ rather than estimating the autocorrelation samples $R_x[m]$. Therefore, the Burg's reflection coefficients, which have been shown in (Campisi et al., 2011) to achieve better performance than the most commonly employed AR coefficients, are here employed.

Given the generic user u , and the generic channel c , let us indicate with $\zeta^{(u,c)}$ the vector, of length Q , composed by the AR model reflection coefficients K_q , for $q = 1, \dots, Q$, using the Burg method:

$$\zeta^{(u,c)} = [K_1^{(u,c)}, K_2^{(u,c)}, \dots, K_Q^{(u,c)}]^T. \quad (5)$$

The model order Q has been selected according to the Akaike Information Criterion (AIC) to minimize the information loss in fitting the data. It can be observed in Figure 3(a), that the AIC(Q) function, averaged among subjects and channels, reaches minimum plateau zone for values of Q from 6 to 12. The feature vector \mathbf{x} for the user u is obtained by concatenating the AR coefficients vectors related to the signals obtained from the channels in the set under analysis. The

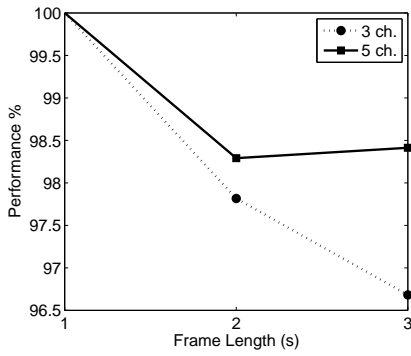


Figure 2: Classification results in % obtained for the best performing set of three (P7-Pz-P8) and five channels (Cz-CP5-CPz-CP6-Pz), considering AR order $Q = 10$ and different values of frame length (T_f).

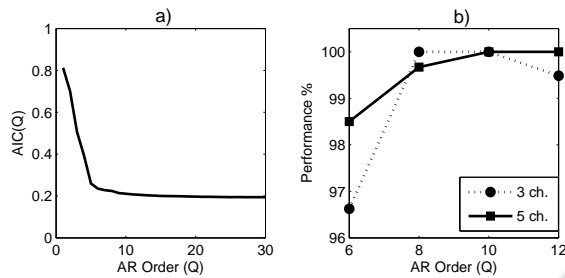


Figure 3: a) AIC function, averaged on all subjects and channels, for the frequency band $[0.5, 30]$ Hz. b) Classification results in % obtained for the best performing set of three (P7-Pz-P8) and five channels (Cz-CP5-CPz-CP6-Pz), considering $T_f = 1s$ and different AR orders Q .

10 AR order has been experimentally selected since it has shown to best fit the EEG data for the recognition purpose, as it can be observed in Figure 3(b), where correct classification percentage is reported considering one second EEG segmentation. Averaged results are shown, obtained training on each session and testing on the remaining one, and considering the best performing sets of three and five channels.

4 CLASSIFICATION

The classifier we propose estimates the class (user identity) to which the observed feature vector \mathbf{x} belongs to by means of a linear transformation $\hat{\mathbf{y}}^T(\mathbf{G}) = \mathbf{x}^T \mathbf{G}$, where the transformation matrix \mathbf{G} is obtained by minimizing the mean square error (MMSE) thus obtaining:

$$\mathbf{G} = \arg \min_{\Gamma} \sum_{i=1}^N p_i \cdot E_{\mathbf{x}|\mathcal{H}_i} \{ [\mathbf{y}_i - \hat{\mathbf{y}}(\Gamma)]^T [\mathbf{y}_i - \hat{\mathbf{y}}(\Gamma)] \} \quad (6)$$

where \mathcal{H}_i indicates the hypothesis \mathbf{x} belongs to the i -th class, with $i = 1, 2, \dots, N$. Here, assuming the hypoth-

esis \mathcal{H}_i holds, the vector $\mathbf{y}_i = [0, \dots, 0, 1, 0, \dots, 0]$ with the unique one in the i -th position, indicates the class i \mathbf{x} belongs to, while $\hat{\mathbf{y}}^T(\mathbf{G})$ represents its estimation. p_i denotes the prior probability that \mathbf{x} belongs to the i -th class. It can be easily shown that the employed optimization criterion given in (6) brings to the normal equations:

$$\mathbf{R}_x \cdot \mathbf{G} = \mathbf{R}_{xy} \quad (7)$$

where $\mathbf{R}_x = E \{ \mathbf{x} \mathbf{x}^T \}$ is the auto-correlation matrix for the elements of the feature vector \mathbf{x} , while $\mathbf{R}_{xy} = \sum_{i=1}^N p_i \cdot E_{\mathbf{x}|\mathcal{H}_i} \{ \mathbf{x} \} \cdot \mathbf{y}_i^T$ turns out to be the matrix whose columns are the probabilistically averaged conditional mean values of the observations \mathbf{x} .

4.1 Dataset

As pointed out in Section 3, different sets of $N_c = 3, 5$ channels, to acquire the signals from which the feature vectors \mathbf{x} is extracted, have been considered for both the employed protocols. Given a chosen set of channels, each of the signals so acquired has been pre-processed, as described in Section 3.1, segmented into N_f frames, and modeled by resorting to the reflection coefficients of an AR model of order Q . Therefore, considering, for each user, EEG signals of duration of 60s, segmented into frames of 1, 2 and 3s, with an overlap factor of 75%, a number of $N_f = 237, 117$ and 77 frames has been obtained respectively, each of which is represented by the feature vector \mathbf{x} of $Q \times N_c$ elements.

Such a set of feature vectors has been collected for each of the two temporally separated recording sessions, 1-3 weeks distant from each other, and each protocol, *i.e.* closed and open eyes resting conditions. It is worth pointing out that the vectors used in the training stage and in the recognition stage have been obtained from the two different acquisition sessions in order to infer about the repeatability over the considered interval of the EEG features for the acquired dataset and the employed acquisition protocols. Hence, we applied the classification algorithm selecting the train and the test datasets without shuffling the EEG frames belonging to different sessions, as performed in other works with user recognition aims. In order to achieve our goal, each one of the two sessions has been sequentially considered for the training dataset while the remaining session has been used to obtain the test dataset, thus obtaining two couples of temporally separated datasets, (training set, recognition set) to train and test the classifier. This kind of validation framework has been provided just to increase the statistical significance of the results. They show that we can't assess a perfect symmetry of changes over time, but that the features keep stable

over the considered interval (1-3 weeks). Results of each test are shown in subsequent columns of Tables 3, and 5 where each set has been acquired at a different time.

4.2 Training

The training stage consists in the estimation of the matrix \mathbf{G} in (7) computed as $\mathbf{G} = \widehat{\mathbf{R}}_{\mathbf{x}}^{-1} \cdot \widehat{\mathbf{R}}_{\mathbf{x}\mathbf{y}}$, where the matrices $\mathbf{R}_{\mathbf{x}}$ and $\mathbf{R}_{\mathbf{x}\mathbf{y}}$ are estimated through MonteCarlo runs, considering equal prior probabilities \mathcal{P}_i for all the classes (users identities) to distinguish between. The estimation was obtained performing the following two sample averages:

$$\begin{aligned}\widehat{\mathbf{R}}_{\mathbf{x}} &= \frac{1}{NM} \sum_{i=1}^N \sum_{m=1}^M \mathbf{x}_{m,i} \mathbf{x}_{m,i}^T \\ \widehat{\mathbf{R}}_{\mathbf{x}\mathbf{y}} &= \frac{1}{NM} \sum_{i=1}^N \sum_{m=1}^M \mathbf{x}_{m,i} \mathbf{y}_i^T,\end{aligned}\quad (8)$$

where $\mathbf{x}_{m,i}$ is the m -th observed feature vector belonging to the i -th class, with M being the number of instances of \mathbf{x} for each class, and $\mathbf{y}_i = [0, \dots, 0, 1, 0, \dots, 0]^T$, with the unique 1 in the i -th position. The considered matrices can be simply upgraded in case of enrollment of N' new users, summing the related matrices $\mathbf{x}_{m,i} \mathbf{x}_{m,i}^T$ to $\mathbf{R}_{\mathbf{x}}$, and adding new columns i to $\mathbf{R}_{\mathbf{x}\mathbf{y}}$ given by $\frac{N}{M(N+N')} \sum_{m=1}^M \mathbf{x}_{m,i}$, where $i = N+1, \dots, N+N'$. To avoid failures and to control accuracy in the estimation of $\mathbf{R}_{\mathbf{x}}^{-1}$, the singular value decomposition based pseudoinversion has been used for the matrix inversion.

4.3 Recognition

In the recognition stage, a linear transformation is applied to each of the $M \times N$ observations from the test dataset. For the i -th user a score vector $\hat{\mathbf{y}}_i$ was obtained for each instance of \mathbf{x}_i in the dataset applying the discrimination matrix \mathbf{G} to $\mathbf{x}_{m,i}$:

$$\hat{\mathbf{y}}_{m,i} = \mathbf{G} \cdot \mathbf{x}_{m,i} \quad (9)$$

with $m = 1, \dots, M$. Subsequently, the M score vectors related to each tested user were summed together to reduce the misclassification error, obtaining

$$\hat{\mathbf{y}}_i = \sum_{m=1}^M \hat{\mathbf{y}}_{m,i}. \quad (10)$$

Finally the estimation of the index representing the user identity is obtained locating the maximum of the score vector $\hat{\mathbf{y}}_i = [\hat{y}_i(1), \dots, \hat{y}_i(N)]^T$ according to the criterion

$$\hat{i} = \arg_l \max y_i(l). \quad (11)$$

5 EXPERIMENTAL RESULTS

An extensive set of experiments has been carried out to test the repeatability of EEG features in the considered interval. Repeatability and stability represent properties of paramount importance for the use of EEG biometrics in real life systems. For this purpose we have selected two simple tasks to be performed by a set of users, and a classification problem has been set up, where the training set and the one to be used in the recognition stage have been chosen belonging to temporally separated sessions 1-3 weeks distant from each other.

More in detail, given the “resting state” acquisition protocols here considered and the 54 employed channels shown in Figure 1, we have considered different subsets of acquisition channels in order to find the best performing spatial arrangements of the electrodes while minimizing their number. Although the considered acquisition technique doesn’t result user convenient, not being this the focus of the paper, in a preliminary study, as this is, it allows to detect on the scalp the brain rhythms which provide the best distinctive features, according to the employed protocol. In order to achieve this goal we have considered sets of three and five electrodes, listed in Tables 3 and 5.

Template extraction has been performed as described in Section 3, by first preprocessing the EEG signals, which includes decimation with sampling rates $S_r = 60$ Hz, CAR spatial filtering, segmentation into frames of T_f s with an overlapping factor O_f between consecutive frames, and eventually band pass filtering in order to analyze the subbands δ, θ, α and β , which are the ones interested by the “resting state” protocols, and some of their combinations. A value of $O_f = 75\%$ has been here employed since we have experimentally proven it is able to guarantee good performance as it provides an adequate sample size to assort the training and recognition datasets. Then the so obtained frames are modeled using an AR model, whose tested orders $Q = \{6, 8, 10, 12\}$ have been estimated by means of the AIC function (see Figure 3(a)). Value of $T_f = 1$ s and $Q = 10$ have been selected as they showed to best characterize the users’ EEG for the recognition task (see Figure 2.)

The template is then obtained by concatenating the reflection coefficients of the signals acquired by means of the electrodes set under analysis, thus generating feature vectors of length $3Q, 5Q$ for the sets of three, and five electrodes respectively.

In Tables 3 and 5 the results obtained for sets of three and five electrodes when using the MMSE classifier, described in Section 4, are given for both employed protocols CE and OE. It is worth pointing out

Table 2: Classification results in % for CE protocol, obtained using the acquisition session t for training and the acquisition session r for recognition, with $t, r = S_1, S_2$ and $t \neq r$, for the subband $\delta \cup \theta \cup \alpha \cup \beta = [0.5, 30]$ Hz, for sets of three electrodes. For each test $t \rightarrow r$ 2 results are provided, considering 75% of the training dataset while 25% (first column) and 75% (second column) of the test dataset.

Electrodes	Closed Eyes							
	Spatial filtering (CAR)				No spatial filtering			
	$S_1 \rightarrow S_2$		$S_2 \rightarrow S_1$		$S_1 \rightarrow S_2$		$S_2 \rightarrow S_1$	
Fp1 Fpz Fp2	51.66	57.57	65.03	69.43	59.87	70.18	65.31	73.42
AF3 AFz AF4	63.43	65.40	66.15	70.79	76.89	91.00	79.23	87.15
F7 Fz F8	50.54	57.76	73.89	82.09	70.32	71.26	78.86	88.65
F3 Fz F4	53.26	59.54	66.34	67.84	59.45	65.54	66.71	69.39
F1 Fz F2	60.81	66.43	74.03	82.56	73.14	85.98	72.95	76.14
FC3 FCz FC4	73.61	81.15	80.45	91.09	77.12	91.14	84.29	94.05
T7 Cz T8	68.26	74.59	70.56	77.12	65.64	59.77	63.90	69.29
C3 Cz C4	78.15	82.51	74.82	85.56	78.57	93.48	84.29	87.39
C1 Cz C2	78.43	88.98	81.81	94.19	80.78	87.01	92.50	99.91
TP7 CPz TP8	65.78	75.34	62.82	57.01	75.06	79.75	80.97	85.61
CP3 CPz CP4	63.62	66.85	59.12	72.95	69.25	71.26	80.03	87.25
P7 Pz P8	93.44	100	94.56	99.62	95.50	100	97.47	100
P5 Pz P6	89.69	99.62	93.25	99.06	80.54	87.01	92.31	100
P3 Pz P4	79.00	79.89	86.08	89.22	67.84	67.93	70.84	78.48
P1 Pz P2	65.07	70.60	62.82	70.79	63.90	63.85	63.06	69.48
PO3 POz PO4	70.98	69.06	77.64	80.87	68.07	81.20	74.07	85.51
O1 POz O2	69.57	74.82	70.70	67.79	69.67	78.43	66.24	70.75

Table 3: Classification results in % for OE protocol, obtained using the acquisition session t for training and the acquisition session r for recognition, with $t, r = S_1, S_2$ and $t \neq r$, for the subband $\delta \cup \theta \cup \alpha \cup \beta = [0.5, 30]$ Hz, for sets of three electrodes. For each test $t \rightarrow r$ 2 results are provided, considering 75% of the training dataset while 25% (first column) and 75% (second column) of the test dataset.

Electrodes	Open Eyes							
	Spatial filtering (CAR)				No spatial filtering			
	$S_1 \rightarrow S_2$		$S_2 \rightarrow S_1$		$S_1 \rightarrow S_2$		$S_2 \rightarrow S_1$	
Fp1 Fpz Fp2	57.48	68.03	67.65	64.65	43.46	49.79	55.41	56.59
AF3 AFz AF4	56.12	56.96	47.12	56.17	53.87	59.21	69.39	73.98
F7 Fz F8	63.57	63.48	67.28	70.18	62.17	67.14	69.67	74.54
F3 Fz F4	66.10	68.17	72.25	70.28	65.78	73.00	60.76	69.01
F1 Fz F2	66.01	66.67	67.23	70.98	54.62	58.37	67.28	69.10
FC3 FCz FC4	83.97	87.15	78.57	87.11	66.99	68.45	67.56	65.96
T7 Cz T8	87.06	83.68	84.11	89.59	76.79	77.03	75.25	80.97
C3 Cz C4	80.08	90.53	78.20	80.87	76.84	81.58	69.48	77.92
C1 Cz C2	72.39	73.65	73.65	82.37	65.45	65.17	69.85	81.20
TP7 CPz TP8	53.26	53.91	58.74	66.29	52.23	55.09	58.09	62.59
CP3 CPz CP4	63.24	72.53	62.96	65.17	75.43	82.00	60.29	63.90
P7 Pz P8	55.32	56.54	59.82	64.70	59.17	60.85	51.24	47.30
P5 Pz P6	53.21	54.99	62.59	64.32	65.07	66.67	53.59	54.71
P3 Pz P4	53.73	57.99	68.59	76.32	79.93	85.33	67.74	76.65
P1 Pz P2	55.79	51.34	59.45	66.76	68.40	74.87	56.82	60.29
PO3 POz PO4	51.76	49.41	55.37	52.23	56.02	63.01	56.26	60.76
O1 POz O2	52.13	48.76	54.85	54.15	54.81	56.02	56.49	61.46

Table 4: Classification results in % for CE protocol, obtained using the acquisition session t for training and the acquisition session r for recognition, with $t, r = S_1, S_2$ and $t \neq r$, for the subband $\delta \cup \theta \cup \alpha \cup \beta = [0.5, 30]$ Hz, for sets of five electrodes. For each test $t \rightarrow r$ 2 results are provided, considering 75% of the training dataset while 25% (first column) and 75% (second column) of the test dataset.

Electrodes	Closed Eyes							
	Spatial filtering (CAR)				No spatial filtering			
	$S_1 \rightarrow S_2$		$S_2 \rightarrow S_1$		$S_1 \rightarrow S_2$		$S_2 \rightarrow S_1$	
FCz T7 Cz T8 CPz	86.31	89.26	82.75	91.80	76.09	76.23	78.67	76.65
FCz C5 Cz C6 CPz	91.05	97.47	88.98	91.14	88.51	94.23	93.34	96.20
FCz C3 Cz C4 CPz	84.90	93.48	83.50	92.73	85.47	97.37	88.05	93.86
FCz C1 Cz C2 CPz	86.69	99.25	84.76	96.67	89.64	98.12	90.67	100
Cz TP7 CPz TP8 Pz	81.67	88.89	80.08	78.62	81.81	88.89	88.98	100
Cz CP5 CPz CP6 Pz	93.44	96.30	95.22	100	94.98	100	96.62	100
Cz CP3 CPz CP4 Pz	93.11	96.30	81.53	89.45	91.28	100	88.94	95.97
Cz CP1 CPz CP2 Pz	96.30	100	93.81	98.03	93.67	95.08	91.65	100
CPz P7 Pz P8 POz	95.78	98.87	94.75	97.84	93.91	100	94.70	97.23
CPz P5 Pz P6 POz	87.62	90.39	91.37	96.39	83.36	94.51	91.70	98.69
CPz P3 Pz P4 POz	81.15	87.11	84.95	87.48	79.51	87.34	84.20	87.29
CPz P1 Pz P2 POz	69.29	75.01	68.82	73.09	65.31	62.96	64.70	72.95
Pz PO3 PO4 O1 O2	68.92	76.00	77.64	94.47	63.48	67.60	77.31	86.12
CPz Pz POz O1 O2	73.23	80.54	76.47	82.51	74.96	75.57	79.75	84.62

Table 5: Classification results in % for OE protocol, obtained using the acquisition session t for training and the acquisition session r for recognition, with $t, r = S_1, S_2$ and $t \neq r$, for the subband $\delta \cup \theta \cup \alpha \cup \beta = [0.5, 30]$ Hz, for sets of five electrodes. For each test $t \rightarrow r$ 2 results are provided, considering 75% of the training dataset while 25% (first column) and 75% (second column) of the test dataset.

Electrodes	Open Eyes							
	Spatial filtering (CAR)				No spatial filtering			
	$S_1 \rightarrow S_2$		$S_2 \rightarrow S_1$		$S_1 \rightarrow S_2$		$S_2 \rightarrow S_1$	
FCz T7 Cz T8 CPz	84.01	79.93	88.05	88.89	79.75	78.90	82.42	87.67
FCz C5 Cz C6 CPz	80.26	75.76	73.98	78.62	70.89	72.90	64.60	70.60
FCz C3 Cz C4 CPz	87.29	88.89	84.29	85.51	73.89	73.56	69.43	73.46
FCz C1 Cz C2 CPz	78.76	81.15	75.95	79.93	69.62	73.42	73.42	80.83
Cz TP7 CPz TP8 Pz	66.39	66.67	59.54	68.78	60.24	59.07	57.06	63.15
Cz CP5 CPz CP6 Pz	68.12	68.21	64.98	66.57	76.75	79.42	71.82	74.87
Cz CP3 CPz CP4 Pz	77.78	86.45	69.48	73.00	74.12	76.84	68.07	71.12
Cz CP1 CPz CP2 Pz	84.58	87.72	71.92	76.51	68.96	71.59	65.73	68.26
CPz P7 Pz P8 POz	67.04	76.14	66.15	69.06	71.68	75.81	61.51	63.90
CPz P5 Pz P6 POz	59.68	59.68	63.95	67.09	62.96	66.67	58.42	56.17
CPz P3 Pz P4 POz	63.43	68.87	65.64	67.09	75.81	77.78	76.23	80.97
CPz P1 Pz P2 POz	65.26	66.48	55.70	57.95	68.82	77.40	61.28	59.49
Pz PO3 PO4 O1 O2	50.45	51.20	53.12	45.94	56.21	55.56	57.34	55.93
CPz Pz POz O1 O2	59.21	59.68	63.48	63.29	55.56	55.56	54.99	58.27

that the signals employed to obtain the templates to be used in both the recognition and the training stage are disjoint in time. Therefore two different combinations of training (t) and recognition (r) sessions, (t, r) with $t, r \in \{S_1, S_2\}$ and $t \neq r$, have been employed in order to infer about the repeatability, over the considered interval, of the EEG features under

analysis, for a real usability of an EEG-based biometric system. Such kind of tests varying the sequence of sessions in the recognition framework are provided to validate the results about repeatability of the features over the interval under analysis. The results for the different tests performed are reported separately, not expecting to make assumptions on symmetry of

Table 6: Classification results in % for both CE and OE protocols, obtained using the same acquisition session S for training and for recognition, with $S = S_1, S_2$, for the subband $\delta \cup \theta \cup \alpha \cup \beta = [0.5, 30]$ Hz, for the best performing sets of three and five electrodes. Results are provided considering 75% of the dataset for training while 25% of the dataset for recognition.

Electrodes	Closed Eyes				Open Eyes			
	Spatial filtering (CAR)		No spatial filtering		Spatial filtering (CAR)		No spatial filtering	
	$S_1 \rightarrow S_1$	$S_2 \rightarrow S_2$	$S_1 \rightarrow S_1$	$S_2 \rightarrow S_2$	$S_1 \rightarrow S_1$	$S_2 \rightarrow S_2$	$S_1 \rightarrow S_1$	$S_2 \rightarrow S_2$
P7 Pz P8	96.81	100	98.03	100	95.22	96.11	94.56	93.25
Cz CP5 CPz CP6 Pz	98.87	100	100	100	100	100	97.00	91.80

changes over time. From Tables 3 and 5, it is possible to note that triplets of channels allow achieving about same performance then configurations employing sets of five channels. This is due to a good spatial localization achieved by configurations of only three sensors, which allow to well capture the underlying phenomena, reducing the problem dimensionality. Moreover, in Tables 3 and 5 results are shown considering the band $F = \delta \cup \theta \cup \alpha \cup \beta = [0.5, 30]$ Hz which is the one that allows obtaining the best results, and considering a preprocessing including CAR filtering or not.

Provided performance refers to a cross-validation framework, obtained selecting for each user 75% of feature vectors \mathbf{x} related to cyclically subsequent frames from the training dataset, while 25% and 75% from the test dataset, as reported in subsequent columns of Tables 3 and 5. Numerical results are obtained averaging over 230 independent cross-validation runs to improve the statistical analysis. As previously pointed out, recognition tests have been carried out keeping independency between the training and the test datasets, acquired in different sessions, for the classification purpose. This aspect is highlighted in Tables 3 and 5 denoting with $S_i \rightarrow S_j$ the result achieved training on S_i and testing on S_j .

It should be noticed that applying the CAR filter in the preprocessing stage doesn't yield a general improvement in the performance for all employed sets of channels and protocols, while it appears to provide best results for some selected channels (FC3-FCz-FC4, C3-Cz-C4, T7-Cz-T8) for sets of 3 channels in the OE protocol. This is likely to be due to artifacts which more affected the open-eyes condition, removed by the spatial filtering. As regards differences between the two employed protocols it is evident, by observing the reported results, that in this experiment the CE protocol provides best performance considering the adopted EEG feature extraction for the recognition task, achieving 100% of correct classification, for example using channels P7-Pz-P8 and 75% of the test feature vectors for each user in the cross-validation framework. This has been observed to be due to being the open-eyes signal more affected by the eyes movement artifacts. It is also worth to be noticed that the combination of channels affected

in a different way the recognition results for CE and OE protocols. In fact, referring to sets of three channels the parietal region has proven to best perform in CE condition, while the central region achieved best results in OE condition. This is in agreement with the fact that in resting state with eyes closed the dominant brain rhythm α can be detected mainly in the posterior area of the scalp, while it is attenuated when opening eyes. Moreover it has been observed, individually analyzing the extracted brain rhythms, that in CE the α band most contributed to the best performance obtained combining all bands ($[0.5, 30]$ Hz). Repeatability over the considered interval of the analyzed EEG features can be inferred by observing that users enrolled in a session have been recognized in a different one, disjoint in time from 1 to 3 weeks. Besides, it is also evident that by swapping the training and recognition roles of the session datasets, that is by considering (t, r) or (r, t) , quite coherent performance are obtained. Finally Table 6 shows results obtained training and testing the classifier on the same session. It should be noticed that very high correct recognition rate is achieved considering just 25% of the test dataset (100% for CE and S_2), while a greater number of feature vectors for each user are needed in the inter-sessions framework. This evidence proves the importance of speculating about the stability and repeatability over time of EEG features for biometric systems.

6 CONCLUSIONS

In this paper the problem of repeatability over time of EEG biometrics, for the same user, within the framework of EEG based recognition, has been addressed. Simple "resting state" protocols have been employed to acquire a database of nine people in two different sessions separated in time from 1 to 3 weeks, depending on the user. Although the dimension of the database employed is contained, we would like to stress out that this contribution represents the first systematic analysis on the repeatability issue in EEG biometrics. As such, this contribution paves the road to more refined analysis which would include more

sessions separated in time as well as different acquisition protocols. Extensive simulations have been performed by considering different sets of electrodes both with respect to their positioning and number. In summary in our analysis a very high degree of repeatability over the considered interval has been achieved with a proper number of electrodes, their adequate positioning and by considering appropriate subband related to the employed acquisition protocol.

REFERENCES

- Abdullah, M., Subari, K., Loong, J., and Ahmad, N. (2010). Analysis of effective channel placement for an eeg-based biometric system. In *Biomedical Engineering and Sciences (IECBES), 2010 IEEE EMBS Conference on*, pages 303–306.
- Barry, R., Clarke, A., Johnstone, S., Magee, C., and Rushby, J. (2007). Eeg differences between eyes-closed and eyes-open resting conditions. *Clinical Neurophysiology*, 118:2765–2773.
- Brigham, K. and Kumar, B. V. (2010). Subject identification from electroencephalogram (eeg) signals during imagined speech. In *Proceedings of the IEEE Fourth International Conference on Biometrics: Theory, Applications and Systems (BTAS'10)*.
- Campisi, P., La Rocca, D., and Scarano, G. (2012). Eeg for automatic person recognition. *Computer*, 45(7):87–89.
- Campisi, P., Scarano, G., Babiloni, F., De Vico Fallani, F., Colonnese, S., Maiorana, E., and L., F. (2011). Brain waves based user recognition using the eyes closed resting conditions protocol. In *IEEE International Workshop on Information Forensics and Security (WIFS'11)*.
- Carmena, J. M. (2012). Becoming bionic. *IEEE Spectrum*, 49(3):24–29.
- Debener, S., Minow, F., Emkes, R., Gandras, K., and de Vos, M. (2012). How about taking a low-cost, small, and wireless eeg for a walk? *Psychophysiology*, 49(11):1617–1621.
- Dornhege, G., del R. Millán, J., Hinterberger, T., McFarland, D., and Möller, K.-R., editors (2007). *Towards Brain-Computing Interfacing*. MIT Press, Cambridge, MA.
- Kay, S. (1988). *Modern Spectral Estimation. Theory and Applications*. Prentice-Hall.
- La Rocca, D., Campisi, P., and Scarano, G. (2012). Eeg biometrics for individual recognition in resting state with closed eyes. In *Proceedings of the International Conference of the Biometrics Special Interest Group (BIOSIG)*, pages 1–12.
- Marcel, S. and del R. Millan, J. (2007). Person authentication using brainwaves (eeg) and maximum a posteriori model adaptation. *IEEE Transactions on Pattern Analysis and Machine Intelligence*, 29(4):743–748.
- McFarland, D., McCane, L., David, S., and Wolpaw, J. (1997). Spatial filter selection for EEG-based communication. *Electroencephalography and Clinical Neurophysiology*, 103(3):386–394.
- Mohammadi, G., Shoushtari, P., Molaee Ardekani, B., and Shamsollahi, M. B. (2006). Person Identification by Using AR Model for EEG Signals. In *Proceedings of World Academy of Science, Engineering and Technology*, volume 11, pages 281–285.
- Nakanishi, I., Baba, S., and Miyamoto, C. (2009). Eeg based biometric authentication using new spectral features. In *ISPACS 2009*, pages 651–654.
- Palaniappan, R. and Patnaik, L. M. (2007). Identity verification using resting state brain signals. In Quigley, M., editor, *Encyclopedia of Information Ethics and Security*, pages 335–341. IGI Global.
- Paranjape, R., Mahovsky, J., Benedicenti, L., and Koles, Z. (2001). The electroencephalogram as a biometric. In *Canadian Conference on Electrical and Computer Engineering*, pages 1363–1366.
- Poulos, M., Rangoussi, M., Chrissikopoulos, V., and Evangelou, A. (1999). Parametric person identification from the eeg using computational geometry. In *The 6th IEEE International Conference on Electronics, Circuits and Systems, 1999. ICECS '99.*, volume 2, pages 1005–1008.
- Riera, A., Soria-Frisch, A., Caparrini, M., Grau, C., and Ruffini, G. Unobtrusive biometric system based on electroencephalogram analysis. *EURASIP J. Adv. Signal Process.*
- Schwartz, M. and Andrasik, F. (2003). *Biofeedback: A Practitioner's Guide*. Guilford Press.
- Su, F., Xia, L., Cai, A., Wu, Y., and Ma, J. (2010). Eeg-based personal identification: from proof-of-concept to a practical system. In *Pattern Recognition (ICPR 2010), 20th International Conference on*, pages 3728–3731.
- Zhao, Q., Peng, H., Hu, B., Liu, Q., Liu, L., Qi, Y., and Li, L. (2010). Improving individual identification in security check with an eeg based biometric solution. In *Proceedings of the 2010 international conference on Brain informatics, BI'10*, pages 145–155, Berlin, Heidelberg. Springer-Verlag.